19th Australasian Fluid Mechanics Conference
Melbourne, Australia
8-11 December 2014

Numerical Investigation of The Behaviour of Wall Shear Stress in Three-Dimensional Pulsatile Stenotic Flows

S. Li[1], C. Chin[1], J. Monty[1], P. Barlis[2], I. Marusic[1], and A. Ooi[1]

[1]Department of Mechanical Engineering, Melbourne School of Engineering
[2]Department of Medicine
The University of Melbourne, Victoria 3010, Australia

Abstract

This paper presents a numerical study of the behaviour of wall shear stress (WSS) in three-dimensional pulsatile flow through an axisymmetric stenosed artery. A realistic blood flow rate (250 ml min^{-1} at rest in coronary artery [7]) and cardiac cycle (T=0.84s [5]) are applied in the simulations. The flow is fully three-dimensional, and the fluid is assumed to be Newtonian and incompressible. Direct numerical simulation (DNS) of the Navier-Stokes equations is carried out to investigate how different levels of stenosis (S) affect WSS. It has been found that larger values of S lead to higher WSS in the stenosis region due to the faster flow velocity at the throat (smaller cross-sectional area). Downstream of the stenosis region, WSS decreases due to viscous effects and remains nearly constant for lower stenosis level cases (S=30% and 50%). However, at the highest stenosis case (S=90%), the WSS distribution becomes unsteady downstream of the throat due to the instabilities in the shear layer.

Introduction

Atherosclerosis, also known as atherosclerotic disease, is the most common form of cardiovascular diseases and the direct cause of heart-attack in the community. It is caused by the formation of plaque on the inner wall that narrows and hardens a specific region in an artery of the human cardiovascular system, which is clinically known as stenosis ([3] and [1]). It was reported by Caro et al [2] that WSS fluctuates rapidly in the vicinity of the stenosis and is relatively steady in other regions of the artery. Since then, various investigations on how the presence of stenosis in the artery affects WSS have been carried out.

In these investigations, one common observation has been noted that blood flow characteristics, such as flow velocity, pressure and WSS, of the post-stenotic region are significantly affected and cause the development of flow recirculation and the formation of vortex rings. It was also reported by Ooi et al [4] that the altered blood flow characteristics (velocity, pressure and WSS) downstream of stenosis may further promote the growth of the stenosis or develop a new stenosis region, as well as the blockage of smaller arteries and hence possibility of plaque rupture.

Apart from the effects of the stenosis, the pulsatile nature of the cardiac cycle is another important factor that influences the flow characteristics in arteries. Several studies have been undertaken to better understand the flow features in pulsatile flow. [4] reported that some researchers have conducted both experimental and DNS study of a pulsatile flow in a constricted pipe and identified that the flow variables are dependent on the inflow conditions upstream of the stenosis. In [4], 2D simulations were carried out to investigate the effects of different stenosis levels. It was found in [4] that, larger stenosis levels result in higher WSS values. Likewise, the formation and propagation of vortex rings are observed and lower stenosis degrees lead to a closer distance between the two subsequent vortex rings. However, only a few studies have considered the numerical study of WSS in three-dimensional pulsatile flow as the simulations are expensive requiring many grid points to fully resolve all spatial and temporal scales in the calculations.

Here, the main purpose is to study how the distribution and behaviour of WSS are affected by varying the stenosis degree in a fully three-dimensional flow field. Specifically, numerical simulations are carried out for an axisymmetric stenosis model with different degrees of stenosis and one pulsatile period. Details of the simulations are described below.

Numerical Model

In this study, the flow is fully three-dimensional, and the fluid is assumed to be Newtonian and incompressible. Thus, direct numerical simulation (DNS) of the incompressible Navier-Stokes equations is carried out to investigate how different levels of stenosis (S) affect WSS.

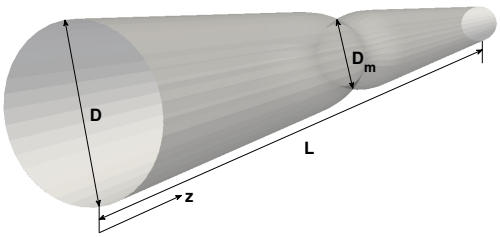

Figure 1. Geometry parameters of the numerical model, where z represents flow direction

The geometry of the stenosed artery is idealised as a smooth constriction on a long rigid straight axisymmetric pipe. The important parameters for this problem are the cross-sectional area of the pipe, $A = \frac{\pi \times D^2}{4}$ and the cross-sectional area of the throat, $A_m = \frac{\pi \times {D_m}^2}{4}$ (see Fig.1), which determine the degree of stenosis,

$$S = \frac{A - A_m}{A} \tag{1}$$

The flow at four different stenosis levels (S=30%,50%,70% and 90%) are investigated. A reference case S=0% is also simulated. All simulations are carried out at Reynolds number $Re_D = \frac{\rho \overline{U} D}{\mu} = 703$, where $\rho = 1000$ kg m^{-3}, $\overline{U} = 0.5896$ m s^{-1}, full pipe diameter, $D = 0.003$ m, and $\mu = 2.5 \times 10^{-6}$ mPa.s, that is within the expected physiological Reynolds numbers measured in vivo [6]. The inlet flow velocity takes the form of the Womersley profile with the cardiac cycle T=0.84s to simulate realistic blood flow for someone at rest (see Fig.2). The same form, but with a shorter pulsatile period (T=0.3s) inlet condition is applied on the same stenosis level case to study the effect of the pulsatile period for a person doing exercise. The Womersley number ($\alpha = r\sqrt{\frac{f\rho}{\mu}}$), which is a dimensionless expression of

the pulsatile flow frequency in relation to viscous effects, for the pulsatile waveforms are 2.59 (T=0.84s) and 4.34 (T=0.3s), respectively. The length of the computational domain is L=20D. For all the cases, the throat of the stenosis is located at 5D from the inlet. The instantaneous WSS distributions are investigated at t_{peak}=1/6T, t_{middle}=11/21T and t_{trough}=37/42T as indicated in Figure 2.

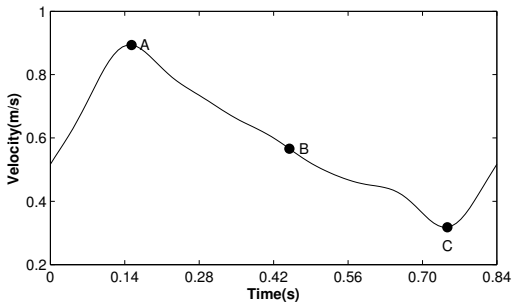

Figure 2. Pulsatile inflow velocity profile (T=0.84s) A: t_{peak} B: t_{middle} C: t_{trough}

The DNS is conducted using an open source CFD code OpenFoam. The size of time step is δt=0.002s. The mesh resolutions close to the wall surface are $\Delta z=1.56\times10^{-5}m$ and $\Delta r=7.8125\times10^{-6}m$, whereas computational Δz and Δr in the middle of the pipe are $1.25\times10^{-4}m$ and $6.25\times10^{-5}m$, respectively. The number of grid points in the models ranges from 3.53×10^{7} to 3.63×10^{7}.

Results and Discussion

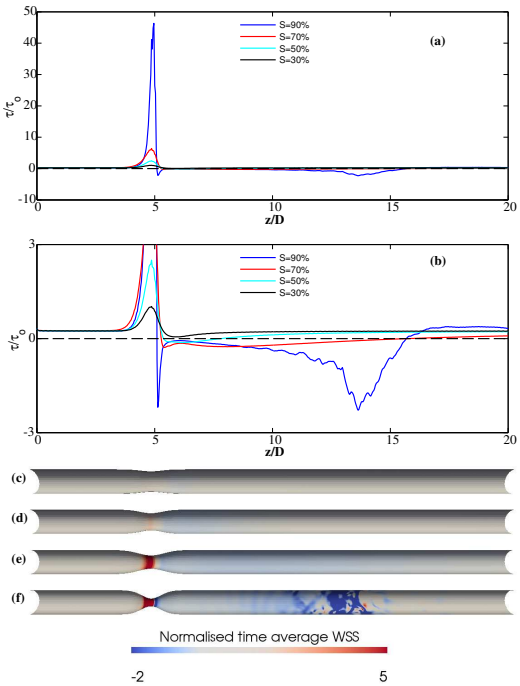

Figure 3. (a) Normalised time average WSS ($\tau\backslash\tau_0$) distributions for different stenosis levels (b) Zoom in figure of (a) with y limits from -3 to 3 (c) S=30% (d) S=50% (e) S=70% (f) S=90%

The time average WSS distributions for different stenosis levels within one cardiac period are displayed in Figure 3. The average values are calculated for one complete period. The results are normalised with τ_0 ,which is the time averaged WSS for S=0%. Upstream of the stenosis, the values of WSS are nearly identical, indicating that WSS is not influenced by the degree of stenosis prior to the stenotic region. At the throat, the results show a positive correlation between the maximum mean WSS and the increase of S. Downstream of the stenosis, the regions of negative WSS are observed in all cases except for S=30%. This shows that the mean recirculation region occurs for all cases except S=30%. There is also a chaotic region for S=90% between z/D=10 and 15, corresponding to the turbulent features of the flow.

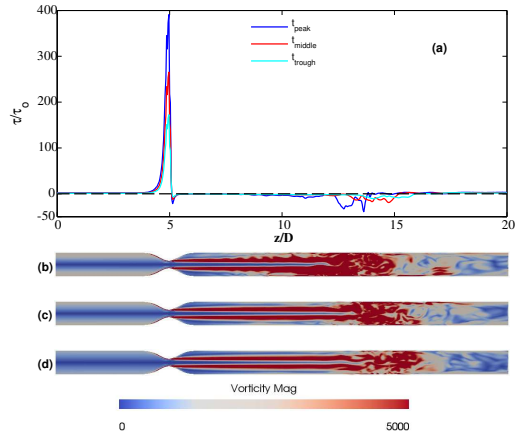

Figure 4. Vorticity magnitude for the pulsatile flow for S=90 % (a) Normalised spatial WSS distributions (b) t_{peak} (c) t_{middle} (d) t_{trough}

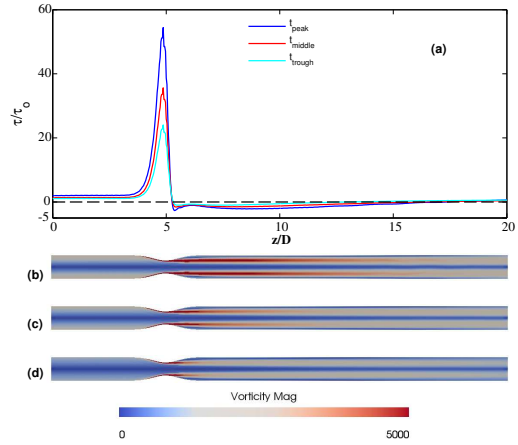

Figure 5. Vorticity Magnitude for the pulsatile flow through the S=70 % model (a)Normalised spatial WSS distributions (b) t_{peak} (c) t_{middle} (d) t_{trough}

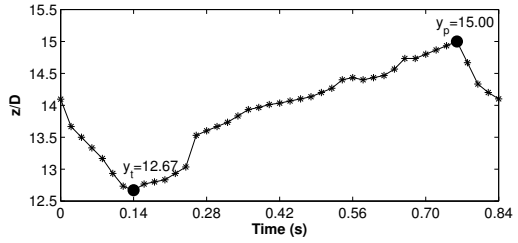

Figure 6. Instantaneous location of the centre of the chaotic region

The instantaneous WSS for different stenosis levels and corresponding vorticity structures are investigated to better understand the influence of the degree of stenosis on the flow field. The vorticity structures for S=90% and 70% at t_{peak}, t_{middle} and t_{trough} are shown in Figs 4(b), 4(c), 4(d) and 5(b), 5(c), 5(d),

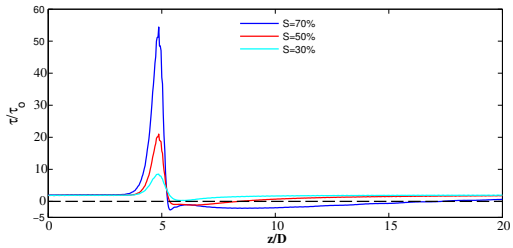

Figure 7. Normalised instantaneous WSS distributions for S = 30, 50, and 70% at t

respectively. Only one period is shown because the flow is periodic. In the vicinity of the throat, a cylindrical shear layer is formed leading to a jet in the proximal of the post-stenotic region. The magnitude of vorticity in the shear layer gradually decreases due to the action of viscosity. For the S=90% case, the shear layer eventually breaks down forming a chaotic region downstream of the stenosis, with turbulent flow characteristics. In [8], the localised turbulent region was also observed in their study. However, it seems here a different mechanism of flow breakdown is observed. In this study, it appears that growth in instabilities in the shear layer eventually leads to chaotic turbulent flow further downstream from the throat, whereas in [8], the breakdown was caused by the tilting of vortex rings formed at the throat.

For S=70%, the shear layer formed at the throat remains steady right through the computational domain. For other cases with lower values of S, the features of vorticity structure are similar to the 70% case in the post-stenotic region.

In both [4] and [8], the formation and propagation of vortex rings were observed in their simulations. [4] investigated three cases from a low stenosis degree of 25% to a high degree of 75% at Reynolds number Re_D=400. The domain specified in S=25% and 75% are 25D and 50D,respectively. Likewise, in [8], DNS was conducted for both steady and single harmonic pulsatile flow in a smooth axisymmetric 75% stenosis tube with the domain 50D at Reynolds number Re_D=750 and 400, respectively. However, this phenomenon does not occur in any of our cases. This may be due to the longer pulsatile period applied in our study with a smaller Womersley number α=2.6 in comparison with [8], where the Womersley numbers range from α=7.2 to 18.6.

Figure 4(a) and 6(a) show the normalised instantaneous WSS at three time steps. The maximum WSS occurs at the stenosis region due to acceleration through the throat. By comparing the data, WSS in S=90% is much greater than that in S=70% because of the small constricted cross-sectional area at the throat.

In the proximal of the post-stenotic region, WSS drops dramatically from positive to negative, indicating a localised but strong recirculation region. Further downstream, the jet becomes unstable and the flow becomes turbulent. The WSS is negative within the chaotic region. Also, the correlation between the location of the vortex breakdown and inlet condition shows that a greater instantaneous inlet velocity leads to a shorter distance between the turbulent region and the stenosis. This correlation is clearly demonstrated in Figure 2, which shows the inlet velocity, and Figure 6 which shows the centre location of the instability region at each 0.02s time step in one period. As indicated in Figure 6, the domain of the chaotic region occurs between 12.67 and 15 z/D.

For S=70%, the chaotic region is no longer observed in the post-stenotic area of the artery model, demonstrating that only a high stenosis level (greater than 70%) could lead to a formation of the chaotic region within the specified domain downstream of the stenosis. Instead, a long domain of recirculation region occurs downstream of the stenosis. As shown in Figure 5, the domain with negative WSS is approximately 5 to 15 z/D. By comparing the data, the recirculation domain at t_{peak} is longer than those at the other two time steps (t_{middle} and t_{trough}), which indicates that greater inlet velocity results in a longer recirculation area. Meanwhile, as indicated in Figures 5(b), 5(c), 5(d), a longer recirculation domain leads to a slower decay of the vorticity strength due to the effect of viscosity.

Figure 7 displays the normalised instantaneous WSS distributions for S=30, 50 and 70% at one specific time step. It is clear that with the decrease of the stenosis level, the length of the recirculation domain decreases accordingly. Also, at S=30%, the WSS across the entire artery model are positive, which implies that the recirculation region at a low stenosis level no longer occurs.

Comparision Between Two Different Womersley Numbers

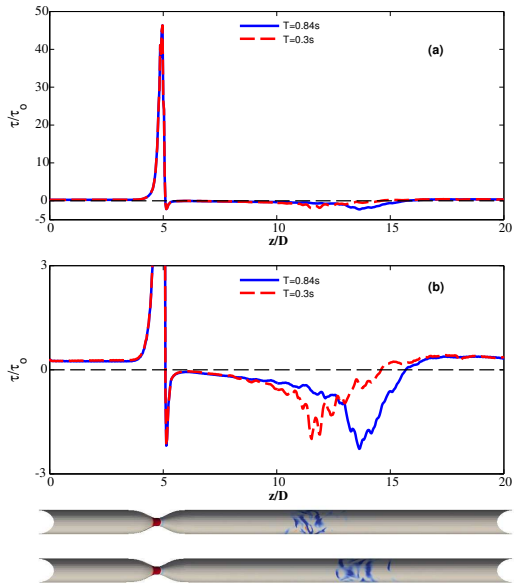

Figure 8. (a) Normalised time average WSS distributions at S=90% for T=0.3s and 0.84s,respectively (b) Zoom in figure of (a) with ylimits from -3 to 3

The effect of the cardiac cycle period in the stenosis artery is investigated by comparing the data with the same form of pulsatile inlet velocity condition but using two cardiac cycles (α=2.59 for T=0.3s and α=4.34 for T=0.84s) for the same stenosis level and mean Reynolds number $Re_D = \frac{\rho \bar{U} D}{\mu} = 703$.The results in Figure 8 show that the distributions of WSS for the two different pulsatile cycles are similar. For S=90%, downstream of the stenosis, the localised instability region occurs closer to the stenosis with the shorter cardiac cycle (T=0.3s). Also, it has been shown that within the instability region ,the WSS magnitude is higher with a longer cardiac cycle. For S=50%, upstream of the stenosis, the WSS magnitude is higher for T=0.3s case. Downstream of the stenosis, the domain of recirculation region in the post-stenotic area with T=0.3s is slightly shorter and the WSS after passing the trough point of the WSS curves are greater than those with T=0.84s, meaning that a shorter cardiac cycle results in a shorter recirculation region in the post-stenotic region, as well as higher WSS.

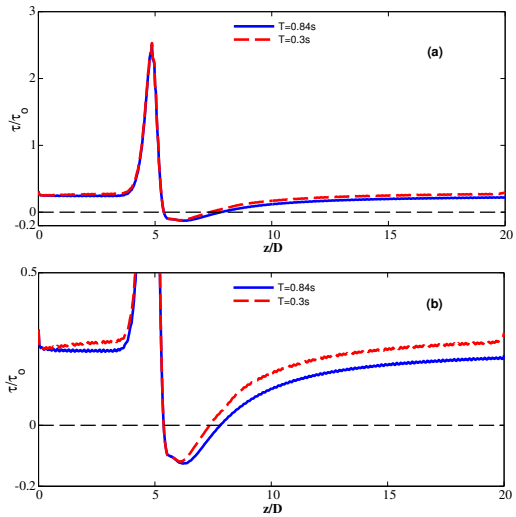

Figure 9. (a) Normalised time average WSS distributions at S=50% for T=0.3s and 0.84s,respectively (b) Zoom in figure of (a) with y limits from -0.2 to 0.5

Conclusions

The objective of this study is to understand the WSS behavior in three-dimensional stenotic pulsatile flow. Direct numerical simulations (DNS) are carried out in an asymmetric stenotic model at four different stenosis levels. Higher stenosis levels lead to greater WSS at the stenotic region. In higher stenosis case (S=90%), the localised turbulent WSS distribution is observed downstream of the stenosis with negative WSS values, indicating the recirculation region. However, this phenomenon does not occur in the lower stenosis cases in the computational domain used here. Instead, the stable negative WSS region after the stenosis is observed. At the low stenosis levels, the length of the recirculation region becomes smaller for lower stenosis levels and eventually disappears.

The effect of the pulsatile boundary condition is also investigated by comparing the results with two different cardiac cycles applied to the same stenosis level. A shorter pulsatile period (T=0.3s) leads to a closer distance between the instability region and the stenosis in the higher stenosis level case. For lower stenosis levels, a shorter pulsatile period results in a shorter length of the recirculation region.

Future studies should focus on the validation of the flow breakdown mechanism in our study and the understanding of vortex ring formation and propagation. The relationship between the breakdown mechanisms with different Reynolds and Womersley numbers should be investigated.

Acknowledgements

The authors would like to thank the Australian Research Council (ARC) Linkage Project scheme and Medtronic. This research is also supported by the VLSCI under grant number VR0210 on its peak computing facility at the University of Melbourne.

References

[1] Boron, W. F. and Boulpaep, E. L., *Medical Physiology, 2e Updated Edition: with STUDENT CONSULT Online Access*, Elsevier Health Sciences, 2012.

[2] Caro, C., Fitz-Gerald, J. and Schroter, R., Atheroma and arterial wall shear observation, correlation and proposal of a shear dependent mass transfer mechanism for atherogenesis, *Proceedings of the Royal Society of London. Series B. Biological Sciences*, **177**, 1971, 109–133.

[3] Corban, M. T., Eshtehardi, P., Suo, J., McDaniel, M. C., Timmins, L. H., Rassoul-Arzrumly, E., Maynard, C., Mekonnen, G., Quyyumi, A. A., Giddens, D. P. et al., Combination of plaque burden, wall shear stress, and plaque phenotype has incremental value for prediction of coronary atherosclerotic plaque progression and vulnerability, *Atherosclerosis*, **232**, 2014, 271–276.

[4] Ooi, A., Blackburn, H., Zhu, S., Lui, E., Tae, W. et al., Numerical study of the behaviour of wall shear stress in pulsatile stenotic flows, in *Australasian Fluid Mechanics Conference*, 2007, volume 12, 2, 2.

[5] Pagani, M., Lombardi, F., Guzzetti, S., Rimoldi, O., Furlan, R., Pizzinelli, P., Sandrone, G., Malfatto, G., Dell'Orto, S. and Piccaluga, E., Power spectral analysis of heart rate and arterial pressure variabilities as a marker of sympathovagal interaction in man and conscious dog., *Circulation research*, **59**, 1986, 178–193.

[6] Radu, M., Pfenniger, A., Räber, L., de Marchi, S., Obrist, D., Kelbæk, H., Windecker, S., Serruys, P. and Vogel, R., Flow disturbances in stent-related coronary evaginations: a computational fluid-dynamic simulation study., *EuroIntervention: journal of EuroPCR in collaboration with the Working Group on Interventional Cardiology of the European Society of Cardiology*.

[7] Ramanathan, T. and Skinner, H., Coronary blood flow, *Continuing Education in Anaesthesia, Critical Care & Pain*, **5**, 2005, 61–64.

[8] Sherwin, S. and Blackburn, H. M., Three-dimensional instabilities and transition of steady and pulsatile axisymmetric stenotic flows, *Journal of Fluid Mechanics*, **533**, 2005, 297–327.